Measurement Based Study of Commercial 5G Frequencies in Urban Macro Cellular Environment

Muhammad Usman Sheikh*, Norshahida Saba*, Lauri Mela*, Jari Salo†, Kalle Ruttik*, Riku Jäntti*
*Department of Communications and Networking, Aalto University 02150 Espoo, Finland
†Elisa Oyj, Helsinki, Finland
Email: {muhammad.sheikh, norshahida.saba, lauri.mela, kalle.ruttik, riku.jantti}@aalto.fi, and jari.p.salo@elisa.fi

Abstract*—Propagation characteristics of different frequency bands have a fundamental impact on the network planning aspects of practical cellular systems. A reasonable understanding of the radio propagation characteristics is already established and well-known large-scale propagation models are available for sub-6 GHz frequencies of operation. However, it is not true for a commercially available band of 26 GHz for fifth-generation (5G) of mobile systems in Europe, and better and accurate path loss models are required. In this research work, we carried out comprehensive continuous wave (CW) channel measurements at three potential 5G frequencies i.e., 1.9 GHz, 3.8 GHz, and 26 GHz in the city of Porvoo, Finland. The existing macrocellular base station (BS) site location is utilized during the measurement campaign. The large bandwidth available at 26 GHz makes it a feasible solution for fixed wireless access (FWA). The coverage achievable by these three bands was evaluated by fitting the alpha-beta-gamma (ABG) and close-in (CI) free space model to the measured path loss. This paper presents a link budget with practical considerations for different frequencies. In the light of acquired results, uplink (UL) is found coverage limited at all considered frequencies, and the attained results highlight the possibility of using 26 GHz band for FWA. Although, the outdoor-to-indoor service provisioning is challenging, however, interestingly it is found that around 1 kilometer and half kilometer coverage can be achieved in downlink (DL) at 26 GHz frequency for the use case of FWA and mobile users, respectively, in an outdoor environment.

***Index Terms*—channel measurements, millimeter wave (mmWave), 26 GHz, signal propagation, path loss, 5G.**

I. Introduction

The fifth-generation (5G) networks aim at serving the increasing data demand of the user by offering high data rates and different quality of services. Millimeter-wave (mmWave) communication is an important feature of the 5G system [1]. Currently, the specifications of the 5G system have reached a high level of maturity, and 5G has entered a mass deployment phase. The frequency band $24.25 - 27.5$ GHz is officially reserved by the European Commission for 5G deployment in Europe [2], and particularly this band of frequency has not been sufficiently covered by the researchers. The 26 GHz band commercial deployment is still in a phase of infancy. Higher frequency of operation not only offers increased bandwidth rather it also allows beamforming and provides higher gain with narrow beam [3]. To take the benefit and to exploit the potential of this band, the characterization of radio propagation at 26 GHz band is essential.

The 3^{rd} generation partnership project (3GPP) also carried out a comprehensive study on channel models for frequencies ranging from 0.5 to 100 GHz, and provided large scale path loss models for different environment types in technical report TR 38.901 [4]. Apart from this, numerous measurement campaigns were launched for different frequencies in various environments, and several path loss models have been proposed in the literature [5]–[8], and two of the well-known path loss models are the alpha-beta-gamma (ABG) model and close-in (CI) free space model. According to our knowledge the validation of these channel models for 26 GHz commercial 5G band is still lacking. The radio propagation at 26 GHz band experiences higher path loss, and it also suffers from heavy blockage due to the foliage. For accurate network planning, operators need valid channel models that reflect those impairments in the allocated frequency band by the regulators. Mobile operators use fixed wireless access (FWA) to provide internet access at homes by utilizing wireless technology instead of fixed lines [9]. The FWA at 26 GHz band can offer high download speed or low latency levels comparable to the modern fiber broadband connection.

Earlier, the cellular network infrastructure was mainly established for global system for mobile communication (GSM) operating at 900 MHz and 1.8 GHz frequency. There is a high incentive for reusing the existing infrastructure in terms of savings in capital expenditure and operational cost. From the mobile operator's point of view, it is recommended to use the existing site for upgrading their network with the newer generation of a cellular system, and for deploying another layer at a different frequency band. However, to ensure the same level of coverage at 26 GHz as at sub-6 GHz band, a fairly large number of new sites are needed. An accurate link budget designed with careful consideration provides the maximum allowed path loss (MAPL) in both DL and UL directions.

In this work, we study the feasibility of existing urban macrocellular (UMa) sites for 3.8 GHz and 26 GHz 5G-BS. With this motivation, measurements were carried out by using a sophisticated measurement setup with high accuracy. In this paper, we provide a comparison of channel measurements for 1.9 GHz, 3.8 GHz, and 26 GHz. The measurement data is used to fit the channel model parameters of the CI and ABG model. Moreover, a practical link budget for the 5G system operating at different frequencies is also provided.

Fig. 1. View to Porvoo from the BS antenna location.

II. Measurement Setup and Scenario

A. Measurement Environment

In a country like Finland, the radio environment changes significantly during the different seasons of the year. Therefore, it is important to highlight here that this measurement campaign was carried out during the summertime in the city of Porvoo, located in the southern part of Finland. Measurements were conducted in an UMa environment dominated by heavy foliage as shown in Fig. 1. It can be seen in Fig. 1, that it is an urban residential area without high-rise buildings, mainly overshadowed by woods (forest). The area is covered with three to eight-floor residential buildings and single-floor houses. An existing macrocellular BS site location is used during this measurement campaign, and the transmitter (Tx) was placed on the rooftop of an eight-floor apartment building at the height of 27 m above the ground level.

B. Measurement cases

In the case of sub-6 GHz frequencies i.e., for 1.9 GHz and 3.8 GHz, drive test measurements were conducted with receiver (Rx) antenna mounted on the car at the height of 2 m. Whereas, stationary measurements were performed at 26 GHz. The global positioning system (GPS) antenna was placed on the roof of the car for tracking the route of the measurement. The measurement system collects the samples continuously. However, due to the varying vehicle speed, the density of measurement samples along the measurement route is different. For drive test measurements, the car was driven twice along the same route i.e., one drive for one frequency measurement. In the post-processing of the measurement data, the measurement area is divided into 10×10 m tiles, and the received signal value in each tile is the average of all measurement samples falling in that tile. In our analysis, we have considered only those tiles for which the measurement data from both frequencies i.e., 1.9 GHz and 3.8 GHz is available. Measurements at 26 GHz requires a stationary receiver and a much longer time for measurement. Therefore, the 26 GHz measurement data is available only for fewer positions.

C. Hardware description and specifications

The sub-6 GHz measurement is done with a continuous single-frequency sinus signal. The transmitter side consists of an Anritsu signal generator with an omnidirectional antenna. The signal generator provides a continuous wave (CW) signal with 40 dBm power. Whereas, at the receiving end there is an omnidirectional antenna connected to Rhode & Schwarz (R&S) TSMW universal radio network analyzer. For 26 GHz measurement, we have utilized the same measurement setup as earlier used in our previous work [10], with the exception that in this measurement, all the antennas were omnidirectional. In this measurement, we have adopted the configuration with external amplifiers at the transmitter and receiver. More details about the parameter setting of the measurement at 26 GHz can be found at [10].

D. Calibration and path loss estimation

The calibration error of the instrument is defined as the difference between the actual and the reported values in the datasheets. We have calibrated the measurement equipment, and all the components involved in the measurement process, and the calibration error between each instrument was determined before the measurement. It is important to highlight here that it was noticed during the measurement that mounting the receive antenna on the flat metallic roof of a car cause deviation in the received signal power due to reflection from a metallic car roof. It has been compensated in measurements by considering an additional 3 dB gain. The measured path loss can be estimated from the received signal power by considering gains and losses of the measurement setup as

$$PL = P_{out} + G - P_{in}, \tag{1}$$

$$G = g_{Tx} + g_{Rx} + g_{cal} - l_{cab} + g_{PA} + g_{LNA}, \tag{2}$$

wherein Eq. 1, P_{in} is the measured received power at the input of the spectrum analyzer or network analyzer without considering the noise power at the Rx side, P_{out} is the output power of the signal generator at the Tx side, and G is the total gain of the system. In Eq. 2, g_{Tx} and g_{Rx} are the gains of the transmitting and receiving antenna, respectively, l_{cab} is the combined loss of all the cables used in the measurement setup, g_{PA} is the gain of the power amplifier (PA) used at the Tx side, g_{LNA} is the gain of the low noise amplifier (LNA) used at the Rx side, and g_{cal} is the combined calibration error of all the instruments involved in the measurement setup.

III. Large scale path loss models

Path loss is needed to estimate the coverage of a cellular cell and is required for evaluating a key factor of signal to interference plus noise ratio (SINR). There are empirical, semi-empirical, and deterministic path loss models. Deterministic models are computationally heavy and are more accurate compared with statistical models. However, statistical models like the 3GPP UMa model, the ABG model, and CI free space model are largely used due to their low computational load and yet offer an acceptable level of root mean square error (RMSE) between the measured and predicted path loss. These models provide large-scale path loss over distance at considered frequencies.

In a technical report TR 38.901 [4], the 3GPP provides path loss models for different types of environment for frequencies from 0.5 GHz up to 100 GHz. In TR 38.901, the mean path loss for outdoor users with Tx-Rx separation less than break point distance for urban macro cellular (UMa) environment in line of sight (LoS) and non-LoS (NLoS) condition is given by Eq. 3 and Eq. 4, respectively.

$$PL_{LoS} = 28 + 22\log_{10}(d_{3D}) + 20\log_{10}(f_c) + \sigma_{LoS}^{3GPP} \quad (3)$$

$$PL_{NLoS} = \max(PL_{LOS}, PL'_{NLOS}) \quad (4)$$

$$\begin{aligned} PL'_{NLoS} = {} & 13.54 + 39.09\log_{10}(d_{3D}) + 20\log_{10}(f_c) \\ & - 0.6(h_{UT} - 1.5) + \sigma_{NLoS}^{3GPP} \end{aligned} \quad (5)$$

where PL_{LOS} and PL_{NLOS} are the mean path loss in LoS and NLoS condition, respectively, expressed in dB value, d_{3D} is the three-dimensional (3D) distance between the Tx and the Rx expressed in meter, f_c is the centre frequency in GHz, and h_{UT} is the actual height of the receiver terminal, σ_{LoS}^{3GPP} and σ_{NLoS}^{3GPP} are the shadowing factor in dB for LoS and NLoS condition, respectively. At any given distance the path loss in an outdoor UMa environment PL_{dB}^{3GPP} under 3GPP UMa model is given by Eq. 6, where Pr_{LoS} is the line of sight probability. More detail about the computation of Pr_{LoS} can be found at Table 7.4.2-1 in 3GPP document TR 38.901 [4].

$$PL_{dB}^{3GPP} = Pr_{LoS} \cdot PL_{LoS} + (1 - Pr_{LoS}) \cdot PL_{NLoS}. \quad (6)$$

The ABG model is an extended form of legacy floating-intercept model, and has three coefficients named as α, β and γ [8]. The equation for the ABG model [1] is given as:

$$PL_{dB}^{ABG} = \alpha 10\log_{10}(d_{3D}) + \beta + \gamma 10\log_{10}(f_c) + x_{\sigma}^{ABG}, \quad (7)$$

where PL_{dB}^{ABG} is the path loss in dB, f_C is the centre frequency in GHz, and d_{3D} is the three dimensional Tx-Rx separation expressed in meters. It can be seen in Eq. 7 that the coefficient of α has distance d_{3D} dependence, and the coefficient of γ depends on the carrier frequency. Meanwhile for β is the optimized path loss offset in dB and x_{σ}^{ABG} is the standard deviation (STD) of shadow fading [1], [7] for ABG model.

The CI model uses a well known free-space path loss (FSPL) model at a reference distance of 1 m as a basis, and has only one distance-dependent parameter as shown in Eq. 8.

$$PL_{dB}^{CI} = FSPL_{dB}\mid_{1\text{m}} + n \cdot 10\log_{10}(d_{3D}) + x_{\sigma}^{CI}, \quad (8)$$

$$FSPL_{dB}\mid_{1\text{m}} = 20\log_{10}\left(\frac{4\pi f}{c}\right). \quad (9)$$

wherein Eq. 8, PL_{dB}^{CI} is the mean path loss, $FSPL_{dB}\mid_{1\text{m}}$ is the free space path loss at the reference distance of 1 m, n is the path loss exponent (PLE), d_{3D} is a 3D distance between Tx-Rx in meter, and x_{σ}^{CI} is the shadow fading standard deviation for CI model. Whereas, in Eq. 9, f is the carrier frequency, and c is the speed of light [1].

IV. LINK BUDGET

A link budget analysis is essential to ensure adequate coverage for the planned cellular network. The link budget provides maximum allowed path loss for considered system configuration and environment type. The cell coverage is determined by using the information of MAPL and planning tool or any large-scale path loss model. In this paper, we have considered LTE and 5G system-specific parameters to evaluate a link budget and system coverage on the studied frequencies. Our target is to compare the coverage of LTE and 5G system in outdoor and indoor conditions for both UL and DL directions. Furthermore, a separate link budget for FWA operating at 26 GHz is provided. The sample link budget for different system configurations is shown in Table I.

The regulatory authorities have allocated different channel bandwidths (BWs) at different frequency bands. Due to limited available BW at sub-6 GHz frequencies compared with mmWave bands, a small system BW is available at 1.9 GHz and 3.8 GHz. In Table I, we have assumed 20, 100 and 400 MHz system BW in DL, and 10, 100, and 400 MHz in UL for 1.9, 3.8 and 26 GHz, respectively. Depending upon the system BW, the 3GPP has specified several OFDM carrier spacing or in other words various sub-carrier bandwidth SC_{BW}. We have considered the sub-carrier BW of 15, 30, and 120 kHz for systems operating at 1.9, 3.8, and 26 GHz, respectively. With the given system BW and SC_{BW}, the number of resource blocks Nr_{RB} available in the DL and UL are given in Table I. The total number of sub-carriers Nr_{SC} can be obtained by multiplying the Nr_{RB} by 12. The maximum available path loss PL_{MAPL} in UL/DL can be computed by using Eq. 10, where T_X^{EIRP} is the effective isotropic radiated power (EIRP) of the Tx, P_{Req} is the required signal power at the Rx, and M is the additional planning margin.

$$PL_{MAPL} = T_X^{EIRP} - P_{Req} - M \quad (10)$$

P_{Req} is estimated by using Eq. 11, where P_{TND} is the thermal noise density at room temperature of 293°K, NF_{R_X} is the noise figure (NF) of the Rx equipment, $SINR$ is the required SINR with respect to the required service type, G_{R_X} is the gain of the Rx antenna, L_{CR_X} is the combined loss of all the cables at the receiving antenna, and G_{LNA} is the optional gain of LNA only considered in the UL direction. In TR 38.901, the 3GPP specifies that the NF of the BS is 5 dB, and the NF of the user equipment (UE) is 9 dB and 10 dB for sub-6 GHz and above 6 GHz frequencies, respectively [4]. Generally, a higher data rate is required in DL compared with UL, therefore a higher value of 0 dB SINR is considered in DL compared with -2 dB in UL. To improve the UL link budget at sub-6 GHz band, the received signal at the BS is amplified by LNA, and we have considered $G_{LNA} = 7\,dB$. The cable loss of 2 dB is assumed at the BS. Whereas at 26 GHz the antenna is placed close to the radio module, therefore LNA is not used, and $G_{LNA} = 0\,dB$.

$$\begin{aligned} P_{Req} = {} & P_{TND} + 10\log_{10}(SC_{BW}) + 10\log_{10}(Nr_{SC}) \\ & + NF_{R_X} + SINR + G_{R_X} - L_{CR_X} + G_{LNA}. \end{aligned} \quad (11)$$

TABLE I
LINK BUDGET.

Parameters	Units	LTE 1.9 GHz		5G-NR 3.8 GHz		5G-NR 26 GHz (M)		5G-NR 26 GHz (FWA)	
		DL	UL	DL	UL	DL	UL	DL	UL
Frequency	GHz	1.9	1.9	3.8	3.8	26	26	26	26
Sub-carrier bandwidth (SC_{BW})	kHz	15	15	30	30	120	120	120	120
System bandwidth	MHz	20	10	100	100	400	400	400	400
Number of RB (Nr_{RB})	Qty	100	50	273	273	264	264	264	264
Number of sub-carriers (Nr_{SC})	Qty	1200	600	3276	3276	3168	3168	3168	3168
Temperature	K	293	293	293	293	293	293	293	293
Receiving end									
Thermal noise density (P_{TND})	dBm/Hz	-173.93	-173.93	-173.93	-173.93	-173.93	-173.93	-173.93	-173.93
Sub-carrier noise power	dBm/sc	-132.17	-132.17	-129.16	-129.16	-123.14	-123.14	-123.14	-123.14
Receiver NF (NF_{R_X})	dB	9	5	9	5	10	7	10	7
Noise power at receiver	dBm	-92.38	-99.39	-85.01	-89.01	-78.13	-81.13	-78.13	-81.13
Required SINR ($SINR$)	dB	0	-2.0	0	-2.0	0	-2.0	0	-2.0
Rx antenna gain (G_{R_X})	dBi	2.0	17.0	8.0	20.0	11.0	23.1	17.0	23.1
Cable loss (L_{CR_X})	dB	0	2	0	2	0	0	0	0
Body loss (L_{Body})	dB	3.0	0.0	3.5	0	4	0	0	0
LNA gain (G_{LNA})	dB	0	7	0	7	0	0	0	0
Required signal power (P_{Req})	dBm	-91.4	-123.4	-89.5	-116.1	-85.2	-106.2	-95.2	-106.2
Transmitting end									
Tx configuration	dBm	8×2	1×1	8×4	2×2	8×8	2×2	8×8	8×4
Tx power per antenna (P_{In})	dBm	34	24	34	24	34	23	34	23
Cable loss (L_{CT_X})	dB	2	0	2	0	0	0	0	0
TMA insertion loss (L_{Ins})	dB	0.5	0	0.5	0	0	0	0	0
Body loss (L_{Body})	dB	0	3.0	0	3.5	0	4.0	0	0
Tx antenna gain (G_{T_X})	dBi	17.0	2.0	20.0	8.0	23.1	11.0	23.01	17.0
Peak EIRP (T_X^{EIRP})	dBm	60.6	23.0	66.6	34.5	75.1	39.1	75.1	55.1
Outdoor MAPL									
Slow fading margin (σ)	dB	8.5	8.5	8.5	8.5	8.5	8.5	6.0	6.0
Fast fading margin (ζ)	dB	7.0	7.0	7.0	7.0	3.0	3.0	2.0	2.0
Coverage threshold	dBm	-75.9	-107.9	-74.0	-100.5	-73.7	-94.7	-87.2	-98.2
MAPL (Outdoor)	**dB**	**136.4**	**130.9**	**140.6**	**135.1**	**148.8**	**133.7**	**162.3**	**153.3**
Indoor MAPL									
Average BPL (η) (Old type)	dB	11.7	11.7	12.8	12.8	17.5	17.5	17.5	17.5
Coverage threshold	dBm	-64.2	-96.2	-61.2	-87.7	-56.2	-77.2	-69.7	-80.7
MAPL (Old building type)	**dB**	**124.7**	**119.2**	**127.8**	**122.3**	**131.3**	**116.2**	**144.8**	**135.8**
Average BPL (η) (New type)	dB	22.1	22.1	27.5	27.5	37.5	37.5	37.5	37.5
Coverage threshold	dBm	-53.8	-85.8	-46.5	-73.0	-36.2	-57.2	-49.7	-60.7
MAPL (New building type)	**dB**	**114.4**	**108.8**	**113.1**	**107.6**	**111.3**	**96.2**	**124.8**	**115.8**

In our link budget, the T_X^{EIRP} is computed by using Eq. 12, where P_{In} is the input power per antenna, G_{T_X} is the gain of the Tx antenna, L_{CT_X} is the combined cable loss at the Tx antenna, L_{Ins} is the insertion loss of tower mounted amplifier (TMA) and that is only considered in the DL, and L_{Body} is the human body loss. The physical size of the antenna at the BS is significantly large as compared with the antenna at the UE side. Similarly, a higher input power can be supported at the BS. Due to the small wavelength at higher frequencies, a large number of antenna elements can be integrated into a limited space. Therefore, in our link budget, at BS we have assumed a configuration of 8×2, 8×4, and 8×8 antennas at 1.9, 3.8, and 26 GHz frequencies, respectively. For LTE system, the most commonly used input power for macro BS is 46 dBm [4], therefore, the transmission power per antenna is set to 34 dBm for 8×2 BS antenna element configuration. For 5G-NR, the transmission power per antenna is also 34 dBm. However, due to the larger number of antenna element configurations i.e., 8×4 and 8×8, the peak EIRP is higher. Similarly, for UE the transmission power is set to 24 dBm and 23 dBm for sub-6 GHz and above 6 GHz frequencies, respectively as recommended by 3GPP in TR 38.901 [4]. Antenna gain is the function of the number of antennas i.e., the higher the number of antennas the higher is the antenna gain. Considering the antenna modeling parameters for BS and UE given in reference [11], the antenna gain at the Tx and Rx end is computed.

$$T_X^{EIRP} = P_{In} + G_{T_X} - L_{CT_X} - L_{Ins} - L_{Body}, \quad (12)$$

The planning margin M consists of environment and location-specific margins as shown in Eq. 13, where σ is slow fading margin (SFM), ζ is fast fading margin (FFM) and η is building penetration loss (BPL). At sub-6 GHz band we have assumed a 8.5 dB and 7 dB of SFM and FFM, respectively. Whereas, at 26 GHz band, due to large system bandwidth the impact of fast fading is less significant, therefore FFM is reduced to 3 dB. Similarly, in the case of FWA due to lack of mobility, a lower value of SFM and FFM is considered. 3GPP provides an O2I-BPL model for two different building types considering distinct material types and compositions [4], [11]. Here, we have computed the MAPL considering the old building type.

$$M = \sigma + \zeta + \eta \quad (13)$$

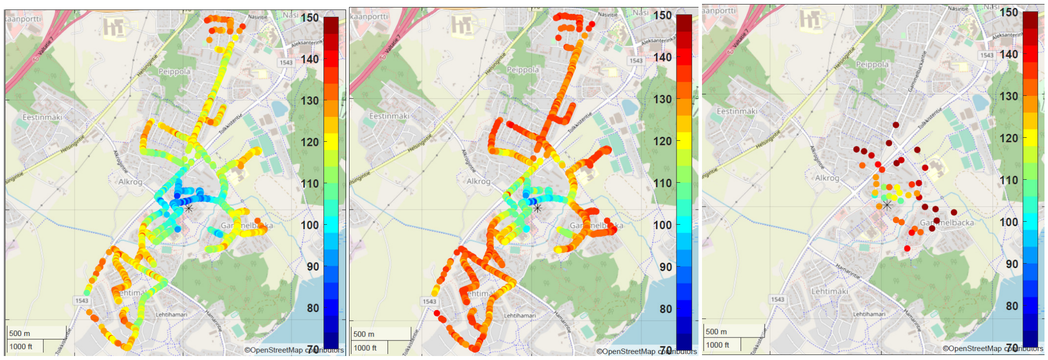

(a) (b) (c)

Fig. 2. Heat map of the measured path loss at different frequencies, (a) 1.9 GHz, (b) 3.8 GHz, and (c) 26 GHz.

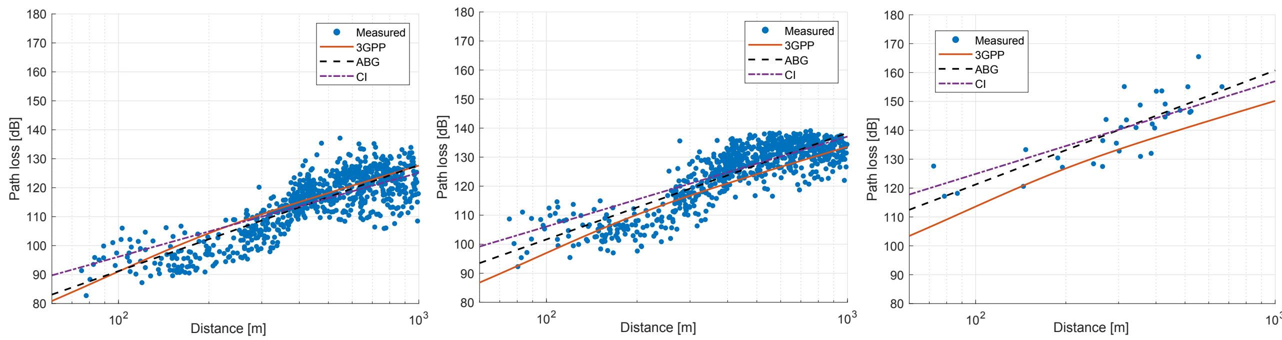

(a) (b) (c)

Fig. 3. Measured and estimated path loss at, (a) 1.9 GHz (b) 3.8 GHz, and (c) 26 GHz.

V. Results and Discussion

Fig. 2 shows the open street map of the area in which the measurements were conducted, and exhibits the heat map of the measured path loss at three considered frequencies. It is important to highlight here that we have considered the samples with NLoS state only for the analysis. In Fig. 2, the position of the Tx is marked with black '$*$', and the color bar shows the value of the path loss in dB scale. As stated earlier that we performed drive test measurements at sub-6 GHz frequencies and stationary measurements at 26 GHz, therefore, a large number of measurement samples i.e., 900 are available for 1.9 GHz and 3.8 GHz frequencies as compared with 40 measurement points at 26 GHz, as shown in Fig. 2. The difference in the path loss values i.e., higher path loss at higher frequencies can be witnessed in Fig. 2. However, for the quantitative analysis of the measurement results, the scatter plot of the measured path loss against the distance is shown in Fig. 3. The estimated path loss with 3GPP, ABG, and CI model is also shown in Fig. 3. It is important to mention here that the three parameters of the ABG model and the PLE parameter of the CI model are obtained by using a curve fitting toolbox of MATLAB, that utilizes the non-linear least square method over measurement data to minimize the RMSE. The acquired values of the ABG and CI model parameters and their corresponding STD are shown in Table II. It was found that for the 3GPP model, the STD increases with the increase in the frequency of the operation. Interestingly, the obtained results reveal that the 3GPP path loss model shows the highest value of the STD among all considered propagation models, and it also shows the largest variation i.e., 5.8–12.0 dB across the considered frequencies. Whereas, the STD of the ABG and CI model varies between 5.4–6.8 dB and 5.6–7.0 dB, respectively, at the studied frequencies. It is important to highlight here that the CI model is the simplest model and has only one parameter to tune, and yet the results acquired with the CI model are quite close to the results obtained through the ABG model. The acquired mean value of the ABG and CI model parameters agree with results reported by Shu Sun et.al [7].

Finally, we used the ABG model along with the MAPL given in Table I to find the coverage of the cell at considered frequencies, for both outdoor and indoor users. Table III shows the maximum coverage distance of a single cell for both DL and UL direction. In the planning process, the MAPL of the limiting link is considered for defining the cell coverage, and the acquired results show that UL is the limiting link at all considered frequencies. Table III shows that in case of LTE 1.9 GHz, the outdoor coverage is estimated as 1285 m, and a reasonable coverage of 821 m can be provided at 3.8 GHz. Interestingly, at 26 GHz in the case of outdoor mobile user an approximately half kilometer coverage can be provided in DL,

TABLE II
LARGE SCALE PATH LOSS MODEL PARAMETERS FOR URBAN MACROCELLULAR NLOS ENVIRONMENT.

Cases	3GPP Model	ABG Model				CI Model	
	σ [dB]	α	β [dB]	γ	σ [dB]	PLE	σ [dB]
1.9 GHz	5.8	3.66	10.15	2.73	5.8	2.9	6.0
3.8 GHz	7.0	3.67	11.37	2.89	5.4	3.1	5.6
26 GHz	12.0	3.95	13.92	2.01	6.8	3.2	7.0

TABLE III
CELL COVERAGE WITH ABG MODEL.

Cell range	Units	LTE 1.9 GHz		5G-NR 3.8 GHz		5G-NR 26 GHz (M)		5G-NR 26 GHz (FWA)	
		DL	UL	DL	UL	DL	UL	DL	UL
Outdoor	m	1820	1285	1161	821	499	208	1097	649
Indoor (Old building type)	m	872	616	520	368	180	75	396	234

whereas the UL is limited to 208 m. It indicates that 26 GHz band can be effectively exploited to provide coverage in a DL direction, and preferably a lower band should be utilized for UL transmission. Furthermore, it is fascinating to find that with given link budget parameters for FWA link, in outdoor a DL coverage of around 1.1 km can be achieved, and it signifies the use of 26 GHz for mobile operators targeting to provide FWA to homes through wireless technology. The acquired results show that O2I service provision is not an issue at 1.9 GHz for old building type, however, O2I signal propagation in a macro cellular environment is quite challenging already at 3.8 GHz, whereas O2I coverage at 26 GHz is cumbersome due to high propagation and penetration loss.

VI. CONCLUSION

We carried out a comprehensive campaign of measurement for commercial 5G frequency bands in an urban macro cellular environment of Porvoo city, Finland. Drive test measurements were done at 1.9 GHz and 3.8 GHz frequencies, and stationary measurements were performed at 40 different locations at 26 GHz. In this paper, we provide a comparison of three well-known path loss models i.e., 3GPP, ABG, and CI. Moreover, a practical radio link budget for LTE and 5G-NR is provided, and also considered a special case of FWA. A non-linear least square method was used to fit the ABG and CI model over the measured data. The acquired results show that the minimum STD was achieved with the ABG model, and the STD of the ABG model varies between $5.4 - 6.8$ dB at the studied frequencies. Interestingly, the CI model with a single tuning parameter offers around 0.2 dB higher STD compared with the ABG model. Whereas, the 3GPP model provides highest STD, around 12 dB at 26 GHz. It is revealed that with the given link budget, the cellular service to an indoor user in an old building type can be supported for a distance up to 370 m at 3.8 GHz. The attained results indicate that 26 GHz band can be effectively exploited to provide coverage of around half a kilometer for a mobile user in a DL direction, and preferably a lower band should be utilized for UL transmission. Furthermore, the obtained results signify the use of 26 GHz for FWA as it is found that a DL coverage of around 1.1 km can be provided while considering a link budget given in this paper.

ACKNOWLEDGEMENT

Special thanks to Elisa Oyj for supporting this work, and it has partial financial support from Academy of Finland project ULTRA (No. 328215) and Business Finland project 5G-Force.

REFERENCES

[1] S. Sun, T. S. Rappaport, S. Rangan, T. A. Thomas, A. Ghosh, I. Z. Kovacs, I. Rodriguez, O. Koymen, A. Partyka, and J. Jarvelainen, “Propagation path loss models for 5G urban micro- and macro-cellular scenarios,” in *2016 IEEE 83rd Vehicular Technology Conference (VTC Spring)*, 2016, pp. 1–6.

[2] European Commission to harmonise the last pioneer frequency band needed for 5G deployment, 14 May 2019. European Commission. [Online]. Available: https://ec.europa.eu/digital-single-market/en/news/european-commission-harmonise-last-pioneer-frequency-band-needed-\5g-deployment

[3] T. S. Rappaport, Y. Xing, G. R. MacCartney, A. F. Molisch, E. Mellios, and J. Zhang, “Overview of millimeter wave communications for fifth-generation (5G) wireless networks—with a focus on propagation models,” *IEEE Transactions on Antennas and Propagation*, vol. 65, no. 12, pp. 6213–6230, 2017.

[4] 3GPP, “Study on channel model for frequencies from 0.5 to 100 ghz,” 3rd Generation Partnership Project (3GPP), Technical Report (TR) 38.901, 12 2019, version 16.1.0.

[5] J. Ko, Y. Cho, S. Hur, T. Kim, J. Park, A. F. Molisch, K. Haneda, M. Peter, D. Park, and D. Cho, “Millimeter-wave channel measurements and analysis for statistical spatial channel model in in-building and urban environments at 28 GHz,” *IEEE Transactions on Wireless Communications*, vol. 16, no. 9, pp. 5853–5868, 2017.

[6] T. S. Rappaport, G. R. MacCartney, M. K. Samimi, and S. Sun, “Wideband millimeter-wave propagation measurements and channel models for future wireless communication system design,” *IEEE Transactions on Communications*, vol. 63, no. 9, pp. 3029–3056, 2015.

[7] S. Sun, T. A. Thomas, T. S. Rappaport, H. Nguyen, I. Z. Kovacs, and I. Rodriguez, “Path loss, shadow fading, and line-of-sight probability models for 5G urban macro-cellular scenarios,” in *2015 IEEE Globecom Workshops (GC Wkshps)*, 2015, pp. 1–7.

[8] M. B. Majed, T. A. Rahman, O. A. Aziz, M. N. Hindia, and E. Hanafi, “Channel characterization and path loss modeling in indoor environment at 4.5, 28, and 38 GHz for 5G cellular networks,” *International Journal of Antennas and Propagation*, vol. 2018, p. 9142367, 2018. [Online]. Available: https://doi.org/10.1155/2018/9142367

[9] E. Oproiu, I. Gimiga, and I. Marghescu, “5g fixed wireless access-mobile operator perspective,” in *2018 International Conference on Communications (COMM)*, 2018, Conference Proceedings, pp. 357–360.

[10] N. Saba, L. Mela, M. U. Sheikh, K. Ruttik, J. Salo, and R. Jäntti, “Measurements at 5G commercial 26 GHz frequency with above and on rooftop level antenna masts in urban environment,” in *2021 IEEE 93th Vehicular Technology Conference (VTC-Spring)*, 2021, pp. 1–5.

[11] 3GPP, “Study on radio access technology: Radio frequency (RF) and co-existence aspects,” 3rd Generation Partnership Project (3GPP), Technical Report (TR) 38.803, 09 2017, version 14.2.0.